An Enhanced Cohesive Crack Element for XFEM using a Double Enriched Displacement Field

J.F. Mougaard, P.N. Poulsen & L.O. Nielsen
Department of Civil Engineering, Technical University of Denmark

ABSTRACT: Applying the principles of the eXtended Finite Element Method a partly cracked cohesive element is developed. The element is based on a double enrichment of the standard displacement field, which allows the element to model equal stresses at the both sides of the crack in the crack-tip element. The formulation is implemented for the 3 node constant strain triangle. A general stress calculation in the cracked elements is presented, the principle is based on an area weighting of the stresses in the cracked elements, which gives a continuous transition to the uncracked respectively the fully cracked element. The performance of the developed element is tested in a Three Point beam Bending Test, where the partly cracked element gives a good over all structural response. Furthermore the partly cracked element gives results without the often seen zigzag behavior on the load-deflection curve.

1 INTRODUCTION

When analyzing discrete cohesive crack growth the eXtended Finite Element Method (XFEM) (Belytschko and Black 2003) is an effective tool with its ability to contain a discrete jump in the displacement field and thereby allowing crack growth without remeshing. As pointed out by (Jirasek and Belytschko 2002) XFEM has some clear advantages compared to the Embedded crack models, especially the ability to model independent displacements and strains in the separated parts.

Applying fully cracked XFEM elements the strains are modeled independently on each side of the crack except for the element containing the tip. In the tip-element the displacement discontinuity must vanish at the edge where the tip is located, see figure 1. This is secured by setting the discontinuity degrees of freedom (DOF) equal to zero at this edge, leaving a reduced number of DOF's for modeling of the strains in the tip-element.

For the CST element only one DOF is active and therefore the case where equal strains and stresses are present at both sides of the crack cannot be modeled, see figure 2(a). This lack of modeling capability in the tip-element is inflicting on the stress distribution in the vicinity of the crack tip. This causes a zigzag crack pattern and also the overall load-displacement response will suffer and the result is some zigzag behaviour, see e.g. (Asferg et al. 2006b). A partly remedy for this problem is to apply a non-local concept for the determination of the stresses.

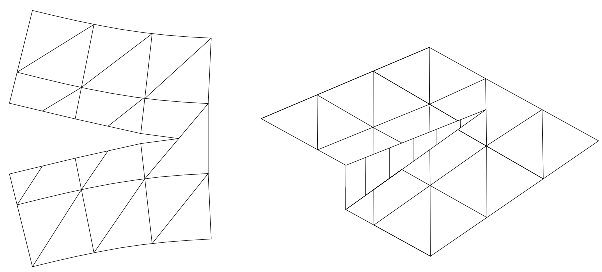

(a) (b)

Figure 1: Discrete discontinuities in deformed finite element meshes. a) Real deformations in plane stress b) Deformations shown perpendicular to the undeformed element mesh

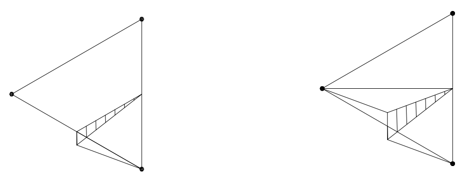

(a) (b)

Figure 2: Discontinuous displacement fields in tip element a) One enriched DOF b) Two enriched DOFs

When e.g. applying an arclength procedure for the solution of the nonlinear problem it is essential to be able to determine a solution in equilibrium at any stage on the load-displacement path. Therefore it is necessary to be able to model the crack-tip at any position in the mesh and thereby the need for a partly cracked XFEM element is evident.

A crack-tip element has been proposed by (Chen 2003), and further developed by (Zi and Belytschko 2003). In this work an appealingly simple displacement field has been suggested however as for the fully cracked element only one discontinuity DOF is active when considering CST element. The element is therefore not able to model equal stresses on both sides of the crack. A direct handling of the lacking modeling capabilities has been presented by (Asferg et al. 2006a) for the CST element by suggesting a displacement field based on an additional enrichment, whereby the element is able to model the same stress on both sides of the crack. By this approach a smooth crack path and load-displacement curve is obtained. The generalization of the work by Asferg to higher order elements has turned out to be difficult. Therefore a new approach is suggested in which the additional enrichments appear in a more systematic way. The resulting additional enrichments for the CST element are identical for the work by Asferg and the present formulation but the generalization to higher order elements is more direct in the present formulation. In the present formulation the element can be used both as partly and as fully cracked.

2 CONCEPTUAL MODEL

2.1 Displacement field

The displacement field is defined in two parts a continuous and a discontinuous. The two contributions is introduced in the standard FEM notation as

$$\mathbf{u}(\boldsymbol{\zeta}) = \mathbf{N}^c(\boldsymbol{\zeta})\mathbf{v}^c + \mathbf{N}^d(\boldsymbol{\zeta})\mathbf{v}^d \qquad (1)$$

Where $\mathbf{u}$ is the displacement vector, $\mathbf{N}^c$ is the continuous interpolation matrix, $\mathbf{N}^d$ is the discontinuous interpolation matrix, $\mathbf{v}^c$ is the continuous DOF vector and $\mathbf{v}^d$ is the discontinuous DOF vector.

The discontinuous part of the displacement field is defined on the basis of the known continuous displacement field, which automatically makes it fulfill the general compatibility rules. A further restriction is introduced. The discontinuous part is not allowed to have any contributions on the element boundary towards non enriched elements. This restriction makes the group of enriched elements compatible with the surrounding standard elements, and ensures that only enriched DOFs are needed in cracked elements.

To fulfill the zero condition on the boundary for the discontinuous displacement field, a modification is needed. This is introduced through the Heaviside step function. If an element is divided into two parts by a crack, the Heaviside function H_{ND} for the respective node ND is defined to be zero on the same side of the crack as the node. The discontinuous interpolation is introduced in a node wise multiplication of the continuous interpolation with such Heaviside functions

$$\mathbf{N}^d(\boldsymbol{\zeta}) = \sum_{ND} H_{ND}(\boldsymbol{\zeta})\mathbf{N}^c_{ND}(\boldsymbol{\zeta}) \qquad (2)$$

Thereby the discontinuous displacement field becomes zero on the boundary. This can be visualized in one dimension, as shown in figure 3.

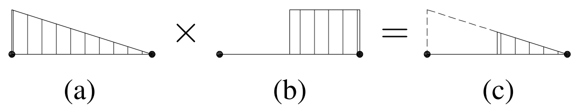

Figure 3: Introduction of a discontinuity in one dimension; (a) the standard displacement field, (b) the Heaviside step function, (c) the discontinuity with the value of zero at the outer boundary

2.2 Double enriched triangular element

When a partly cracked element is introduced it is important that the element can model two independent stresses at the crack-tip, see figure 2(b). Furthermore the formulation for the fully and the partly cracked element should be compatible. This will allow the crack to propagate with a continuously growing DOF-vector.

As mentioned, the fully and partly cracked tip elements by (Zi and Belytschko 2003) had only one discontinuous DOF to model the stress state at the crack-tip when considering CST elements, see figure 2(a). In order to model equal stresses at both sides of the crack at the crack-tip a further enrichment of the displacement field is needed, see figure 2(b).

This is introduced by an additional triangle defining a second discontinuous displacement field. This principle is shown in figure 4, where the discontinuous displacement field is composed of contributions from the two triangles D1 and D2. The partly cracked case is shown where only two discontinuity DOFs are active. The displacement field is now seen to be able to give equal stresses at both sides of the crack at the crack-tip.

The two introduced discontinuity triangles and the discontinuity itself is sketched in figure 5, where a systematic numbering is introduced.

Each of the two discontinuity triangles have their own set of discontinuity DOFs. In general the two discontinuity triangles gives six shape functions. The fully cracked case is now considered, meaning that

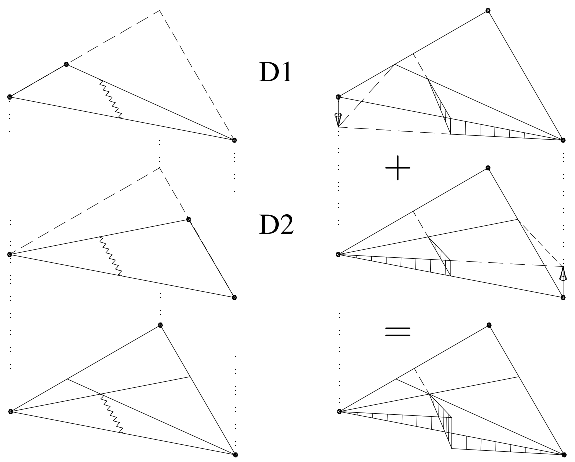

Figure 4: Principle of the double enriched displacement field for the partly cracked CST element.

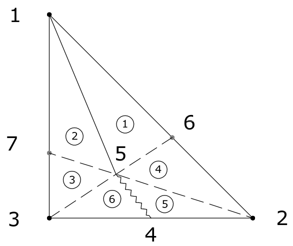

Figure 5: Part and numbering for the partly cracked CST element

part 1,2 and 3 in figure 5 is collapsed. Figure 6 shows the six shape functions, where each of the discontinuity DOFs are set to unity. When the element is fully cracked it is necessary to define on which side of the crack the discontinuity DOF in node 7 is. In this case the same side as node 1 is chosen.

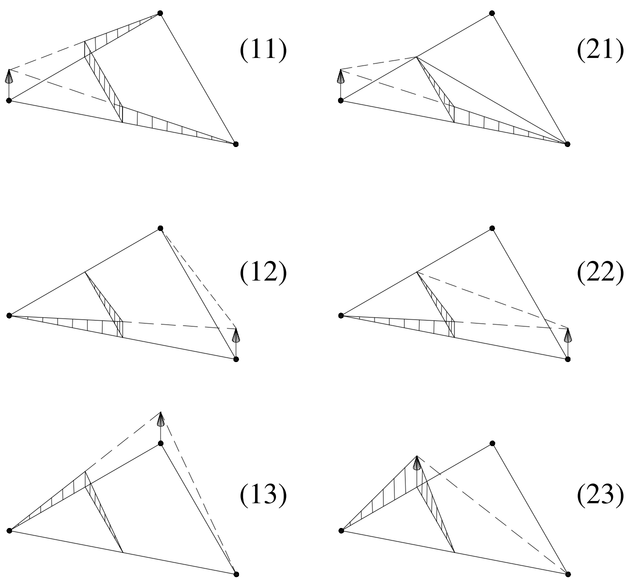

Figure 6: The six shape functions for the double enriched CST-element

Two sets of the presented shape functions are seen to be dependent, meaning that two of them should be cancelled. In this case 22 and 23 are cancelled. The four remaining shape functions are all independent. A closer look at 12, 13 and 21 shows that they are side local, while 11 gives contributions on two boundaries. The four shape functions can be seen as a basis for the discontinuous displacement field i.e. a combination of them will still represent the same basis. Therefore 11 is redefined by subtracting 21 from 11. A new side local basis has now been defined for the discontinuous displacement field, which is shown in figure 7.

The discontinuous DOFs are organized in nodes on the sides of the triangle. Each of these nodes represents a discontinuous shape function as shown in figure 7. When the crack propagates from one element to another only the discontinuity DOFs on the current side activates. This actually shows that the system DOF vector grows continuously.

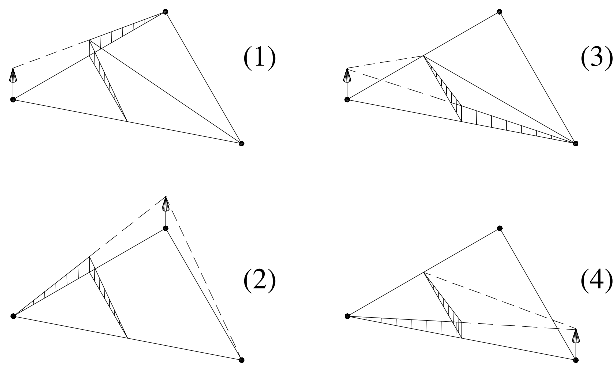

Figure 7: Discontinuous shape functions for the CST element using a side local basis

2.3 Shape functions

In each of the triangles the shape functions are the usual CST shape functions

$$f_1 = \zeta_1 \quad f_2 = \zeta_2 \quad f_3 = \zeta_3 \tag{3}$$

These are determining the displacement contribution in each of the three triangles 123, 237 and 236 shown in figure 5.

2.4 Discrete Cohesive Crack

A discrete cohesive crack is running through the structural domain Ω with the boundary Γ defined in the usual right-handed rectangular coordinate system (x,y,z), in this case a plane stress problem in the xy-plane, as shown in figure 8. A set of definitions are needed. The crack is running from S to T. The general curve from T to S defines the local crack orientation s as tangent to the crack curve and n defines the normal to the crack, where n is set so (n,s,z) is a usual right handed coordinate system. Positive n coordinates defines the positive side of the crack.

At the crack faces the stress state constitutes a normal stress σ_n and a shear stress τ_{ns}, with corresponding opening $\Delta u_n = u_n^+ - u_n^-$ and tangential slip $\Delta u_s = u_s^+ - u_s^-$.

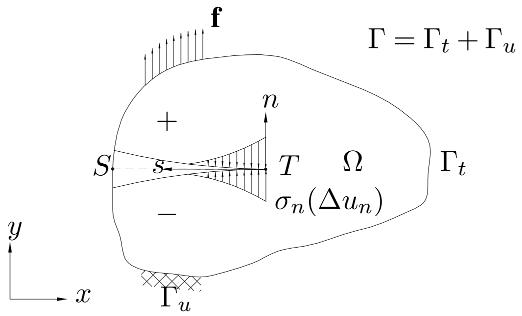

Figure 8: Notation for the implementation of the cohesive crack in a finite element model. Visualized with vanishing shear stresses on the crack faces.

Having the cohesive crack in the FEM model leaves a part of the virtual internal work to be performed in the the crack. This work is done by σ_n with Δu_n and σ_s with Δu_s. This leaves the variational formulation as described below.

2.5 Generalized Stresses and Strains

By looking at the incremental virtual internal work of the uncracked part of the structure the usual format is found

$$\begin{aligned} \delta W^i &= \sigma_x \delta\epsilon_x + \sigma_y \delta\epsilon_y + \tau_{xy}\delta\gamma_{xy} \\ &= \boldsymbol{\sigma}\delta\boldsymbol{\epsilon} \end{aligned} \tag{4}$$

Defining the generalized stress and strain vectors as

$$\boldsymbol{\sigma} = \begin{bmatrix} \sigma_x \\ \sigma_y \\ \tau_{xy} \end{bmatrix} \quad \boldsymbol{\epsilon} = \begin{bmatrix} \epsilon_x \\ \epsilon_y \\ \gamma_{xy} \end{bmatrix} \tag{5}$$

For the crack the incremental internal virtual work is formulated as

$$\begin{aligned} \delta W^i &= \sigma_n \delta\Delta u_n + \tau_{xy}\delta\Delta u_s \\ &= \boldsymbol{\sigma}_{cr}\delta\boldsymbol{\epsilon}_{cr} \end{aligned} \tag{6}$$

Defining the generalized stress $\boldsymbol{\sigma_{cr}}$ and strain $\boldsymbol{\epsilon_{cr}}$ vectors in the crack as

$$\boldsymbol{\sigma}_{cr} = \begin{bmatrix} \sigma_n \\ \tau_{xy} \end{bmatrix} \quad \boldsymbol{\epsilon}_{cr} = \begin{bmatrix} \Delta u_n \\ \Delta u_s \end{bmatrix} \tag{7}$$

2.6 Tangent stiffness matrix

Using the expression for the virtual work a direct formulation of the tangent stiffness matrix for the cracked element can be written.

The total DOF-vector for the element is organized with the continuous DOFs followed by the discontinuous DOFs

$$\mathbf{v} = \begin{bmatrix} \mathbf{v}^c & \mathbf{v}^d \end{bmatrix} \tag{8}$$

For the continuous part of the element the incremental virtual internal work can be formulated as

$$\begin{aligned} W^i_{cont} &= \int_{V_{cont}} \delta\boldsymbol{\epsilon}^T \boldsymbol{\sigma} dV \\ &= \delta\mathbf{v}^T \int_{V_{cont}} \begin{bmatrix} \mathbf{B}_c & \mathbf{B}_d \end{bmatrix}^T \mathbf{D}_T \begin{bmatrix} \mathbf{B}_c & \mathbf{B}_d \end{bmatrix} dV \mathbf{v} \\ &= \delta\mathbf{v}^T \begin{bmatrix} \int_{V_{cont}} \mathbf{B}_c\mathbf{D}_T\mathbf{B}_c dV & \int_{V_{cont}} \mathbf{B}_c\mathbf{D}_T\mathbf{B}_d dV \\ \int_{V_{cont}} \mathbf{B}_d\mathbf{D}_T\mathbf{B}_c dV & \int_{V_{cont}} \mathbf{B}_d\mathbf{D}_T\mathbf{B}_d dV \end{bmatrix} \mathbf{v} \\ &= \delta\mathbf{v}^T \begin{bmatrix} \mathbf{k}_T^{cc} & \mathbf{k}_T^{cd} \\ \mathbf{k}_T^{dc} & \mathbf{k}_T^{dd} \end{bmatrix} \mathbf{v} \end{aligned} \tag{9}$$

Where $\mathbf{D}_T$ is the continuous material tangent stiffness, $\mathbf{k}_T^{cc}$ is the element tangent stiffness contribution from continuous DOFs, $\mathbf{k}_T^{dd}$ is the element tangent stiffness contribution from discontinuous DOFs and $\mathbf{k}_T^{cd}$ and $\mathbf{k}_T^{dc}$ is the element tangent stiffness contribution from the interaction between the continuous and discontinuous DOFs.

Analogous the incremental virtual internal work done in the crack can be formulated as

$$\begin{aligned} W^i_{cr} &= \int_{cr} \delta\boldsymbol{\epsilon}_c r^T \boldsymbol{\sigma}_{cr} ds \\ &= \delta\mathbf{v}^T \int_{cr} \begin{bmatrix} \mathbf{0} & \mathbf{B}_{dd} \end{bmatrix}^T \mathbf{D}_T^{cr} \begin{bmatrix} \mathbf{0} & \mathbf{B}_{dd} \end{bmatrix} ds \mathbf{v} \\ &= \delta\mathbf{v}^T \begin{bmatrix} \mathbf{0} & \mathbf{0} \\ \mathbf{0} & \int_{cr} \mathbf{B}_{dd}\mathbf{D}_T^{cr}\mathbf{B}_{dd} ds \end{bmatrix} \mathbf{v} \\ &= \delta\mathbf{v}^T \begin{bmatrix} \mathbf{0} & \mathbf{0} \\ \mathbf{0} & \mathbf{k}_T^{cr} \end{bmatrix} \mathbf{v} \end{aligned} \tag{10}$$

Where $\mathbf{D}_T^{cr}$ is the crack tangent stiffness matrix and $\mathbf{k}_T^{cr}$ is the element tangent stiffness contribution from the crack.

By summation the total incremental internal virtual work can be found

$$\begin{aligned} W^i &= \delta\mathbf{v}^T \begin{bmatrix} \mathbf{k}_T^{cc} & \mathbf{k}_T^{cd} \\ \mathbf{k}_T^{dc} & \mathbf{k}_T^{dd} + \mathbf{k}_T^{cr} \end{bmatrix} \mathbf{v} \\ &= \delta\mathbf{v}^T \mathbf{K}_T \mathbf{v} \end{aligned} \tag{11}$$

Where $\mathbf{K}_T$ is the element tangent stiffness matrix.

2.7 Inner nodal forces

The internal nodal forces **Q** corresponding to a given displacement state **v** has to be formulated in order to solve the nonlinear equations.

In general this is done using the actual stress level $\boldsymbol{\sigma}$ which here is a function of the displacements. The only nonlinear contribution is from the cracked elements where the cohesive stresses in general have a nonlinear behavior. The nodal forces can for an element be calculated as

$$\mathbf{q} = \int_{el} \mathbf{B}^T \sigma d\Omega \tag{12}$$

For the cracked elements this is formulated using the terms and organization from the previous section as

$$\mathbf{q} = \begin{bmatrix} \int_{el} \mathbf{B}_c^T \boldsymbol{\sigma} d\Omega \\ \int_{el} \mathbf{B}_d^T \boldsymbol{\sigma} d\Omega + \int_{cr} \mathbf{B}_{cr} \boldsymbol{\sigma}_{cr} dS \end{bmatrix} = \begin{bmatrix} \mathbf{q}_c \\ \mathbf{q}_d \end{bmatrix} \tag{13}$$

3 IMPLEMENTATION

3.1 Algorithm

With the definition of the nonlinear problem through $\mathbf{K}_T$ and **Q** a general solution strategy can be chosen. In the present work the orthogonal residual procedure by (Krenk 1999) is used. It is presented in the seudo algorithm below.

initial state: $\mathbf{v}_0, \mathbf{R}_0, \Delta\mathbf{v}_0 = \mathbf{0}, E_{ref}$
load increments $n = 1, 2, \ldots, n_{max}$
  $\Delta\mathbf{v}_1 = \mathbf{K}_{n-1}^{-1} \Delta\mathbf{R}_n$
  $\Delta\mathbf{v} = \mathit{min}(1, v_{max}/\|\Delta\mathbf{v}_1\|)\Delta\mathbf{v}_1$
  if $\Delta\mathbf{v}_0^T \Delta\mathbf{v} < 0$ *then* $\Delta\mathbf{v} = -\Delta\mathbf{v}$, $\Delta\mathbf{R}_n = -\Delta\mathbf{R}_n$
  iterations $i = 1, 2, \ldots, i_{max}$
    $\Delta\mathbf{Q} = Q(\mathbf{v}_{n-1} + \Delta\mathbf{v}) - \Delta\mathbf{R}_{n-1}$
    $\xi = \Delta\mathbf{Q}^T \Delta\mathbf{v} / \Delta\mathbf{R}_n^T \Delta\mathbf{v}$
    $\mathbf{r} = \xi \Delta\mathbf{R}_n - \Delta\mathbf{Q}$
    $\mathbf{K}_{n-1} = \mathbf{K}(\mathbf{v} + \Delta\mathbf{v})$
    $\delta\mathbf{v} = \mathbf{K}_{n-1}^{-1} \mathbf{r}$
    $\delta\mathbf{v} = \mathit{min}(1, v_{max}/\|\delta\mathbf{v}\|)\Delta\mathbf{v}$
    $\Delta\mathbf{v} = \Delta\mathbf{v} + \delta\mathbf{v}$
    $E_i = \frac{1}{2}\mathbf{r}^T \delta\mathbf{v}$
  stop iterations when $E_i < \epsilon_p E_{ref}$
  $\mathbf{v}_n = \mathbf{v}_{n-1} + \Delta\mathbf{v}$
  $\mathbf{R}_n = \mathbf{R}_{n-1} + \xi \Delta\mathbf{R}_n$
  $\Delta\mathbf{v}_0 = \Delta\mathbf{v}$
stop load incrementation when $(\|\mathbf{R}_n\| > \mathbf{R}_{max})$ *or* $n = n_{max}$

Where **v** is the system dof vector, **R** is the system load vector, **K** is the system stiffness matrix, **Q** is the system internal nodal forces, ξ is the residual scaling factor and E_i is residual energy.

As convergence criterion an energy criterion has been applied using the energy in the initial load step as reference E_{ref}. The equilibrium iterations are performed using a general Newton Raphson algorithm. Each time the crack propagates the system stiffness matrix is changed. The stiffness change is so radical that equilibrium cannot be achieved without updating the tangent stiffness.

3.2 Stress calculations

In general the FEM solution does not give a continuous stress distribution in the structure, i.e. stress discontinuities will exist over element borders. Considering the implementation of a cohesive crack in a finite element model these stress discontinuities will play a certain role.

Consider a crack propagation in a structure. The restriction for how long the crack will propagate is determined by the tip stress being equal to the tensile strength, f_t. Therefore stress discontinuities could give an undefined solution over an element border.

In order to get a clearly defined crack propagation in the finite element model, a stress average has to be introduced.

3.3 Nodal mean stresses

Using CST elements a weight function is introduced using nodal mean stresses. These nodal mean stresses gives a well defined stress distribution without any discontinuities, and is therefore a suitable weighting.

This leaves the stress state to vary linearly between the three element nodes. The stress interpolation follows the displacement shape functions for the element. This is a general way of weighting the stresses in the structure in order to achieve stress continuity.

3.4 Nodal Contributions from Elements

Calculating nodal mean stresses is straight forward in the continuous elements using the general relation $\boldsymbol{\sigma} = \mathbf{D}\boldsymbol{\epsilon}$.

The enriched displacement field allows the element to produce three independent stress answers i.e. one from each of the two discontinuous enrichments and one from the continuous displacement field. Combinations of those gives the stress answers in each of the six parts shown in figure 5.

In order to obtain a consistent stress calculation when the crack propagates over element borders, a suitable weighting has to be used in the partly cracked element. Thus the stress answer from the partly cracked element will have to converge to the level for the continuous element when the crack length tends to zero. Further, the stress evaluation will have to fit the other limit case, where the partly cracked element approaches the fully cracked case.

For the CST element, a single stress answer is calculated from each element, even though the enriched displacement field in general allows more than one stress state. The weighting is done using the areas of each part $(A_1, \ldots, A_6)$.

When the partly cracked element approaches the fully cracked case the dominant areas are 4-6 which is the definition of the fully cracked element. When the crack is entering a new element, it is the areas 1-2 that are dominant. Areas 1-2 only contains continuous

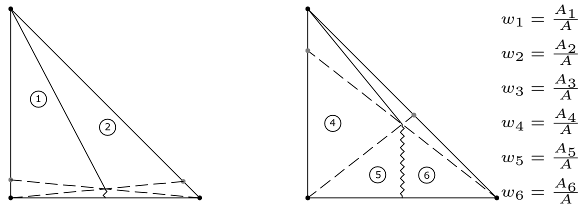

Figure 9: The two limit cases for the partly cracked element - converge against the continuous element and converge against the fully cracked element

contributions i.e. when the crack enters the new element the stress evaluation is based on the continuous stress answer as shown in figure 9.

3.5 Solution strategies

The crack propagation is based on the tangent stiffness in the previous converged state. Setting the crack to propagate perpendicular to the first principal stress direction, the load increment **df** will result in a new stress state with a new tip coordinate extrapolated along the crack propagation line as shown in figure 10.

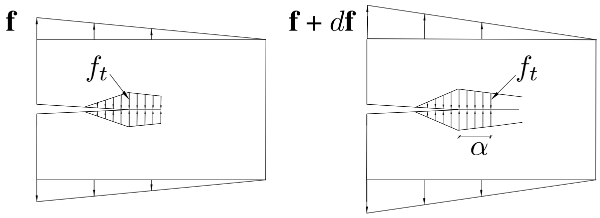

Figure 10: Principle of the crack length extrapolation based on the tangent stiffness in a load step.

Estimating the new tip coordinate as described above does not necessarily give the correct crack length for the applied load increment. After updating the system stiffness with the new crack geometry a new equilibrium state is found by solving the nonlinear equations. This will in general lead to a tip stress different from the estimated f_t level. It is here convenient to introduce the three dimensional coordinate ($\mathbf{f}$,$\boldsymbol{\alpha}$,$\boldsymbol{\sigma}_T$), where **f** represent the load vector, $\boldsymbol{\alpha}$ the crack length and $\boldsymbol{\sigma}_T$ the tip stress.

Solving the system equations gives equilibrium but in general a non physical solution with a tip stress differing from the tensile strength. This is solved by introduction of a tip stress iteration. This tip stress iteration is done either using the crack length or the load factor as iteration parameter.

4 EXAMPLE

One structural example is considered. The purpose is to verify the developed XFEM element. The chosen example is the Three Point Beam Bending Test (TPBT).

The structural example shows the capability of modeling a crack running partly through elements. Furthermore the example proves that the element is capable of capturing the correct overall structural behaviour.

4.1 Geometry and Materials

The geometry of the test specimens has chosen to be in accordance with RILEM recommendations for the TPBT.

Parameters used in this chapter are listed in table 1 and fits a high quality concrete. A linear-traction-separation law has been used in the calculations.

f_t =	3.50	[MPa]	h = 150.00	[mm]
G_f =	160.00	[Nm/m^2]	l = 500.00	[mm]
ν =	0.20	[ ]	w = 150.00	[mm]
E =	37.40	[GPa]		

Table 1: Geometric and material parameters used for the structural example

4.2 Three point beam bending test

The TPBT is considered in two cases, namely a reference specimen without a notch and the standard specimen with a 25 mm notch. The geometry, support and load conditions are shown in figure 11.

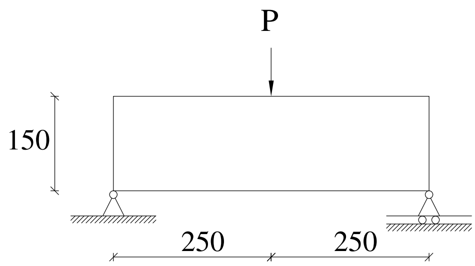

Figure 11: Geometry and support conditions for the TPBT, the point force is split up in two nodal forces applied symmetrically on the center element - the applied mesh is shown in figure 15

4.3 Reference specimen without notch

A reference calculation has been performed on the TPBT without the notch. To avoid influence of other parameters the crack propagation has been forced in a vertical direction. The global structural response is shown in figure 12. In the solution strategy the crack length has been predefined to propagate 1/5 of the element length through three elements approximately located half way up in the beam. A zoomed view of this domain is shown in figure 13.

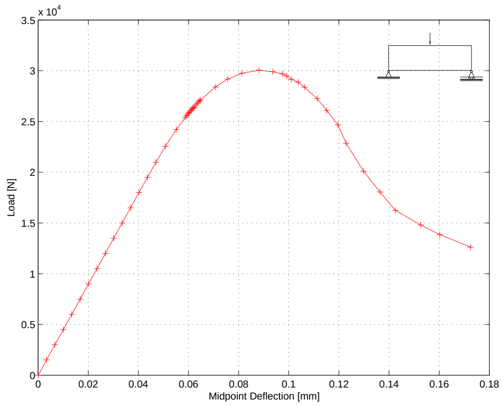

Figure 12: Load-deflection response for the TPBT in the reference case without notch, showing the point load versus the midpoint deflection.

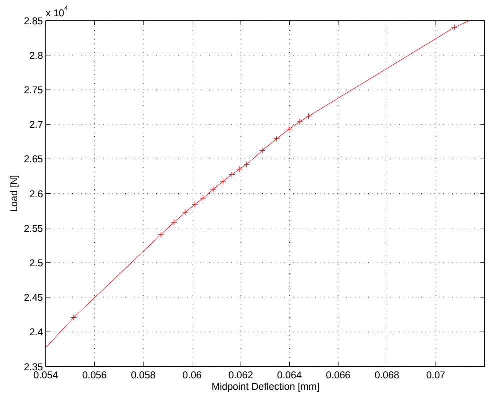

Figure 13: Zoomed view of the load-deflection response, showing the solutions for the crack length in jumps of 1/5 of the element length through three elements approximately located at the midpoint at 1/2 of the beam height

The partly cracked solutions are seen to fit the general structural response in this area. This is one of the primary goals of this work, and shows the capability of modeling continuous crack growth in a finite element model using a partly cracked element with a simple enrichment.

4.4 TPBT Standard Specimen 25mm Notch

TPBT is one of the most used test examples in the literature. Work done by (Asferg et al. 2006a) shows that the solution from the commercial finite element program DIANA, using standard interface elements along a predefined crack, can be accepted as a sufficiently accurate solution. This DIANA computation, is therefore used as a reference for the XFEM modeling.

In figure 14 the reference case without the notch is plotted as well. This is done to verify that the two models converges asymptotically when the crack propagates and gets stress free at the end of the notch.

Comparison with the DIANA solution shows a similar structural response. The present solution exceeds

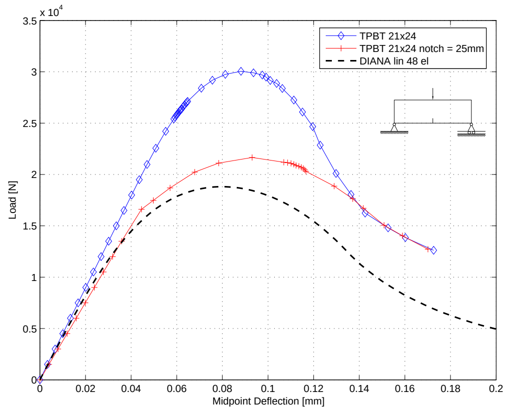

Figure 14: Load-deflection response for the TPBT, showing the point load versus the midpoint deflection.

the peak value with approximately 10-15%. This is mainly explained in the lacking accuracy of the CST element. More elements are needed to provide accurate results, but it is acceptable in the context of testing the general implementation and performance. Using the nodal mean stresses for the tip stress calculations, will typically also overestimate the peak value. This is due to averaging in the surroundings of the crack-tip where the stresses generally are smaller than the tensile strength, whereby the estimated tip-stress is lowered.

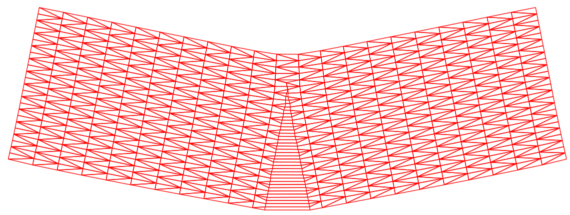

Figure 15: Deformed systemplot, verifying the support and load conditions for the TPBT

When using the provided solution strategy, divergence is typically found when there is approximately 5 uncracked elements left above the crack tip. Using the nodal mean stresses, it will be difficult to fulfill the tip stress criterium when the stress change over the element length becomes too large. The stress state around the crack-tip is shown in figure 16 for the last converged load step.

Based on the computations done in the present work, a general convergence problem is seen when the crack faces at the bottom of the beam reaches the point of being stress free. Around this point the step size reduces see figure 14, leaving the crack to propagate in small steps through the element. These numerical problems are believed to be caused by the large change in stiffness on the linear traction-separation-law, when the stress free crack faces starts to propagate from the bottom of the beam.

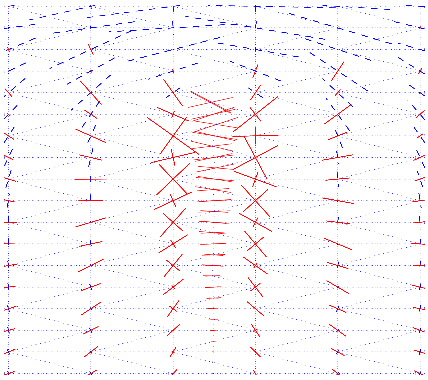

Figure 16: Zoomed view of the principal and crack stresses around the crack tip for the TPBT

5 CONCLUSION

In the present work a double enriched cohesive crack element has been developed based on concepts of the eXtended Finite Element Method (XFEM).

The considered formulation is in plane stress, and is implemented for the CST element. The enriched CST element is formulated generally so it covers both the fully and partly cracked case. Using the double enriched displacement field, both the fully and partly cracked element is capable of modeling equal stresses at the crack-tip.

The developed element is tested in structural example consisting of the Three Point beam Bending Test. A good overall structural response is achieved by comparing the TPBT with results from a reference solution. The peak value is exceeded with approximately 10-15%. This is mainly explained by the rather coarse mesh combined with the accuracy of the CST element. A higher order implementation is needed to get more accurate results still keeping a reasonable low number of elements.

When testing the partly cracked element, it can be concluded that it gives a continuous description of the points between two fully cracked cases on the load-deflection response, which was one of the goals with the general formulation of the cracked element.

The systematic formulation of the displacement field in the present work is believed to be applicable to higher order elements.

REFERENCES

Asferg, J. L., P. N. Poulsen, and L. O. Nielsen (2006a). A consistent partly cracked xfem element for cohesive crack growth. *Accepted in: Int. J. Numer. Meth. Engng*.

Asferg, J. L., P. N. Poulsen, and L. O. Nielsen (2006b). A direct xfem formulation for modeling of cohesive crack growth in concrete. *Submitted in: Computers and Concrete*.

Belytschko, T. and T. Black (2003). Elastic crack growth in finite elements with minimal remeshing. *International Journal for Numerical Methods in Engineering* (45), 601–620.

Chen, H. (2003). *Enriched finite element methods and its applications*. Ph. D. thesis, Northwestern University.

Jirasek, M. and T. Belytschko (2002, July). Computational resolution of strong discontinuities. In J. E. H. A. Mang, F. G. Rammerstorfer (Ed.), *Fifth World Congress on Computational Mechanics*, Vienna, Austria.

Krenk, S. (1999). An orthogonal residual procedure for nonlinear finite elements equations. *International Journal for Numerical Methods in Engineering* (38), 823–839.

Zi, G. and T. Belytschko (2003). New crack-tip elements for xfem and applications to cohesive cracks. *Int. J. Numer. Meth. Engng.* (57), 221–224.